

## Research Article

# Dynamics and Synchronization of a Memristor-Based Chaotic System with No Equilibrium

**Hong-Min Li, Yan-Feng Yang, Yang Zhou, Chun-Lai Li , Kun Qian, Zhao-Yu Li, and Jian-Rong Du**

*College of Physics and Electronics, Hunan Institute of Science and Technology, Yueyang 414006, China*

Correspondence should be addressed to Chun-Lai Li; [hnistlichl@163.com](mailto:hnistlichl@163.com)

Received 26 July 2019; Accepted 17 September 2019; Published 28 October 2019

Guest Editor: Viet-Thanh Pham

Copyright © 2019 Hong-Min Li et al. This is an open access article distributed under the Creative Commons Attribution License, which permits unrestricted use, distribution, and reproduction in any medium, provided the original work is properly cited.

The topics of memristive system and synchronization are two hot fields of research in nonlinear dynamics. In this paper, we introduce a memristor-based chaotic system with no equilibrium. It is found that the memristor-based system under investigation exhibits fruitful dynamic behaviors such as coexisting bifurcation, multistability, transient chaos, and transient quasiperiod. Thus, it is difficult to reproduce the accurate dynamics of the system, which is highly advantageous in encryption and communication. Then, a simple intermittent control scheme with adaptive mechanism is developed to achieve complete synchronization for the introduced system. Because the output signal is transmitted intermittently to the receiver system, more channel capacity can be saved and the security performance can be improved naturally in practical communication.

## 1. Introduction

As the fourth basic circuit element along with resistor, inductor, and capacitor, the memristor was postulated by Chua in 1971 [1], and it was then successfully fabricated by the HP laboratories in 2008 [2]. Since then, the memristor was recognized to perfect the symmetry of the four fundamental circuit variables and has aroused wide interest in academia [3–5]. The memristor is commonly defined as a two-terminal nonlinear component with controllable resistance called memristance that varies according to the amount of charge or flux flowing through it [6]. The fingerprint of a memristor is composed of a current-voltage characteristic curve, which shows a pinched hysteresis loop whose shape varies with frequency and converges to a straight line with the increase of frequency [7].

The memristor is currently used to design flash memory, improve neural networks, and construct chaotic circuits, for the intrinsic characteristics of memory, nanoscale device, and inherent nonlinearity. Itoh and Chua constructed the memristive chaotic oscillator in 2008, by replacing Chua's diodes in Chua's circuit with the piecewise linear memristor

[8]. Afterwards, many memristor-based chaotic oscillators were constructed. For example, by replacing the single diode with a memristor in the original circuit, Pelap postulated an emendatory Tamasevicius oscillator [9]. Bi-Rong designed a simple chaotic circuit consisting of an inductor, a capacitor, and a voltage-controlled memristor [10]. Zhao et al. proposed a memristor-based chaotic system by replacing the nonlinear diode in the Chua circuit with an active flux-controlled memristor [11]. In order to increase the complexity of memristor-based system, Teng et al. used a fourth-degree polynomial memristance to produce a multiscroll chaotic attractor [12]. By replacing Chua's diode with a physical SBT memristor and a negative conductance in the canonical Chua's circuit, a new memristor-based modified Chua's circuit is constructed [13]. There usually emerges special dynamics in this kind of memristive systems, such as initial sensitivity, coexisting bifurcation, coexistence attractors, and transient dynamics. Therefore, the memristive chaotic system will provide more complex dynamics and facilitates the engineering applications of information encryption, secure communication, and signal processing [14–17].

Meanwhile, close attention was paid to chaotic system without equilibrium [18–20]. From the computer-processing perspective, it is challenging to numerically localize the attractor in such system since there is no transient process leading from the vicinity of unstable equilibrium point. In other words, the attracting basin of such system does not intersect with any small neighborhood of its equilibrium point, or the attractor is “hidden” [21–24]. Up to now, little information is known about the dynamical behavior in such system, and what is worse is that the Shilnikov criteria cannot be employed to prove the chaos for the absence of heteroclinic or homoclinic orbit [25, 26].

Because of its application in secure communication, digital signal, neural network, and other fields, the synchronization of chaotic system is a fashionable subject in nonlinear science. Since the first scheme was carried out by Pecora and Carroll for the synchronization of two identical chaotic systems [27], a great diversity of methods have been proposed to synchronize chaotic systems, such as active control, adaptive control, impulsive control, sliding mode control, intermittent control, pinning control, and hybrid control [28–31]. Generally, a chaotic communication system can be constructed based on master-slave synchronization, where the message is modulated by the transmitting system and is then sent to the receiving system. Also, in the receiver, the designed synchronization scheme is used to demodulate the received signal and extract the message [32]. The intermittent synchronization implies that the slave system receives the demodulated information from the master system intermittently. Therefore, the intermittent synchronization scheme will decrease the amount of conveyed information and the communication channel capacity will be reserved for more message transmission. Also, accordingly, the security of the chaotic communication system will be improved since the redundancy of the synchronization information in the channel is reduced. Therefore, the intermittent synchronization scheme is especially fit for the design of practical chaos-based communication system.

In this paper, we introduce a memristor-based chaotic system with no equilibrium. The dynamical evolution of the memristive system is studied by using phase diagram, time-domain trajectory, bifurcation diagram, and Lyapunov exponent. It is found that by changing system parameters or initial condition, the reported system exhibits different topological structures of coexisting bifurcation, multistability, transient dynamics. The coexisting hidden attractors signify that the system has fruitful and complex dynamic behaviors, which is highly advantageous in encryption and communication for the difficulty of reproducing the accurate dynamics of the system. Then, a simple intermittent control scheme with adaptive mechanism is developed to achieve complete synchronization for the introduced memristive system. Since the output signal is transmitted intermittently to the receiver system, more channel capacity can be saved and the security performance of the communication system can be improved naturally in practical communication. Theoretical analysis and illustrative examples are executed to verify the effectiveness of the proposed synchronization scheme.

## 2. Memristor-Based Chaotic System with No Equilibrium

**2.1. Model Description.** Based on Sprott A system, the constructed memristive chaotic system can be described by the following differential equations:

$$\begin{cases} \dot{x} = y, \\ \dot{y} = -Wx + yz, \\ \dot{z} = c - y^2, \end{cases} \quad (1)$$

where  $x, y, z$  are state variables; the function  $W$  represents the model of a flux-controlled memristor, depicted as  $W = 3ax^2 + b$ ; and  $a, b, c$  are positive parameters.

The dissipativity is decided by  $\nabla V = (\partial \dot{x}/x) + (\partial \dot{y}/y) + (\partial \dot{z}/z) = z$ ; thus, system (1) is non-Hamiltonian conservative of phase volume [33]. It is palpable that there exists no equilibrium in system (1). Therefore, the strange attractor is “hidden” in the sense of classification method described by Leonov et al. [21], and the Shilnikov method cannot be employed to verify the emergence of chaos since there is no heteroclinic or homoclinic orbit in this system. It is easy to know that the system is symmetric with respect to the  $y$ -axis in the sense of coordinate transformation  $(x, y, z, t) \rightarrow (-x, y, -z, -t)$ .

When choosing the parameters  $a = 3$ ,  $b = -1$ , and  $c = 1$  and initial condition  $(0.2, 0.15, 0)$ , system (1) appears a chaotic state with the Lyapunov exponents  $0.1062, 0, -0.1062$ , as illustrated by the phase portrait in Figure 1.

**2.2. Coexisting Bifurcation and Multiple Attractors.** It is found that the memristive system under consideration can experience rich bifurcation structures when continuously monitoring the bifurcation parameter. Also, the memristive system has completely different bifurcation behaviors when the initial conditions are set to different values.

We assign the parameters  $b$  and  $c$  of system (1) as  $b = -1$  and  $c = 1$ , and select parameter  $a$  serving as the representative bifurcation parameter. The coexisting bifurcation diagrams, produced by the local maxima of the state variable  $z$  in terms of control parameter  $a$ , are depicted in Figure 2(a) when the system starts with the initial states  $(0.1, 0, 0)$  and  $(0.2, 0, 0)$ . Also, the corresponding maximal Lyapunov exponents are depicted in Figure 2(b). This strategy represents a convenient and intuitive approach to identify the window in which the multiple coexisting attractors arise. We further draw in Figure 3 the enlarged bifurcation diagrams of Figure 2(a) to show the typical regions of multiple coexisting attractors. By taking different initial conditions  $(0.1, 0, 0)$  and  $(0.2, 0, 0)$ , respectively, we plot the coexisting multiple attractors with different parameter  $a$  in Figure 4. It is found that there may emerge rich dynamical structures of coexisting chaos, quasiperiod or period with different shape for the same parameter  $a$  when starting from different initial states.

We also study the dynamics evolution of system (1) by using the initial value  $x(0)$  served as the bifurcation parameter. The system parameters are fixed as  $a = 3$ ,  $b = -1$ ,  $c = 1$ , and the rest initial conditions are assigned to be  $y(0) = 0, z(0) = 0$ . The bifurcation diagram and spectra of

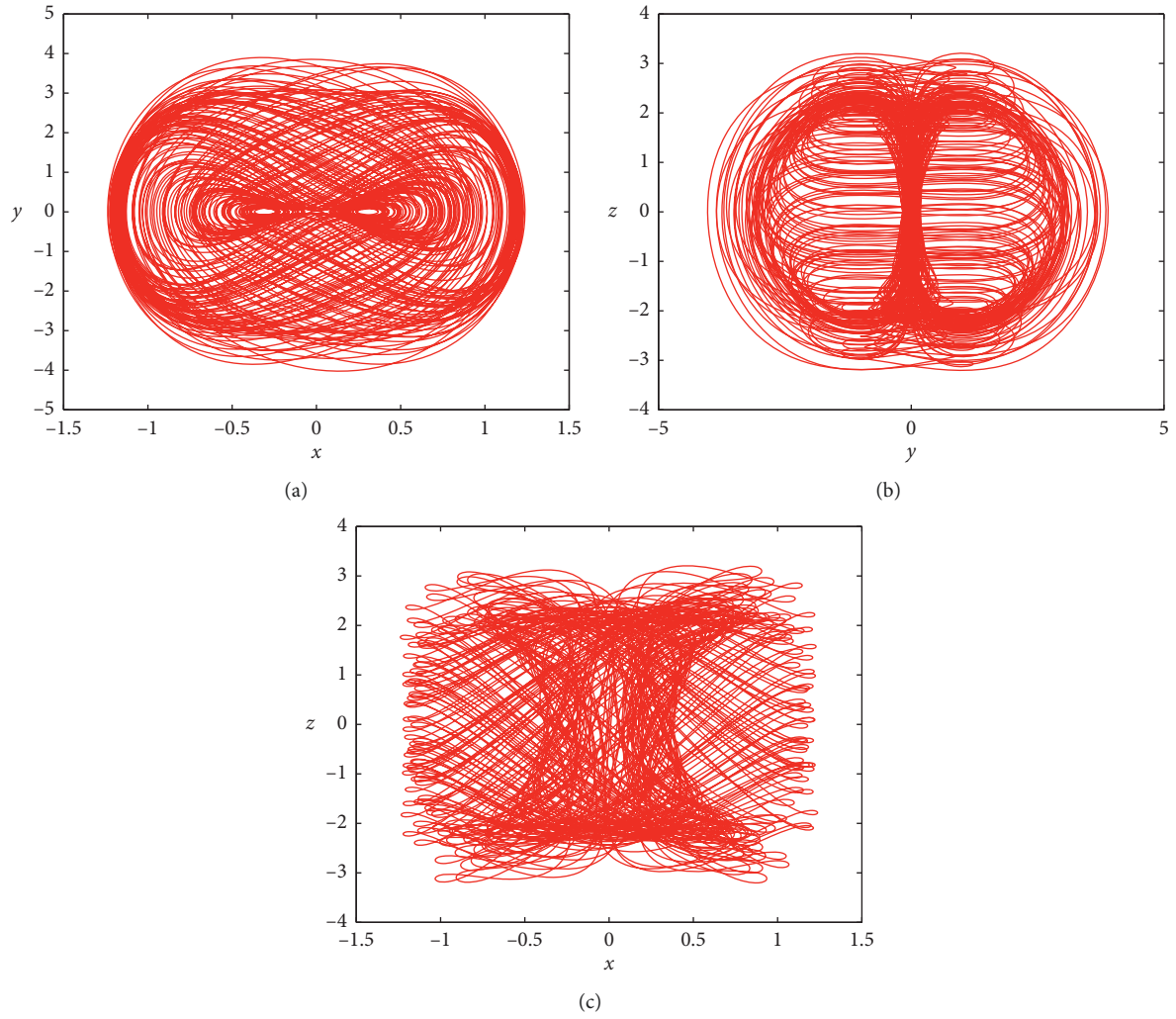


FIGURE 1: Phase portrait projected onto the plane of (a)  $x$ - $y$ ; (b)  $y$ - $z$ ; (c)  $x$ - $z$ .

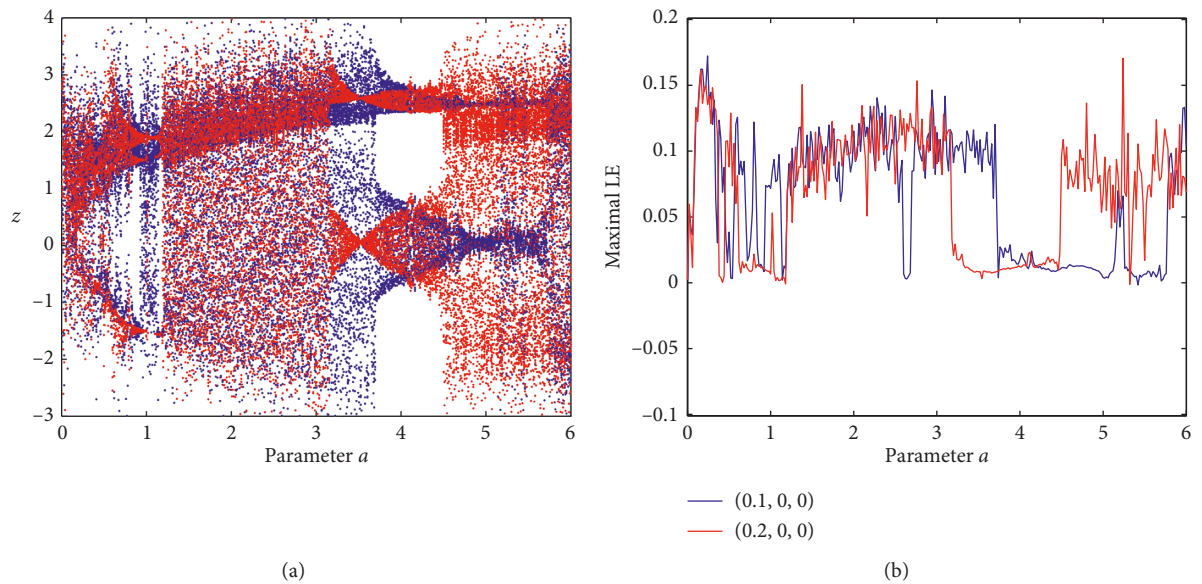


FIGURE 2: (a) Bifurcation diagrams and (b) spectra of maximal Lyapunov exponent versus parameter  $a$ , the initial conditions are (0.1, 0, 0) for blue diagrams and (0.2, 0, 0) for red diagrams.



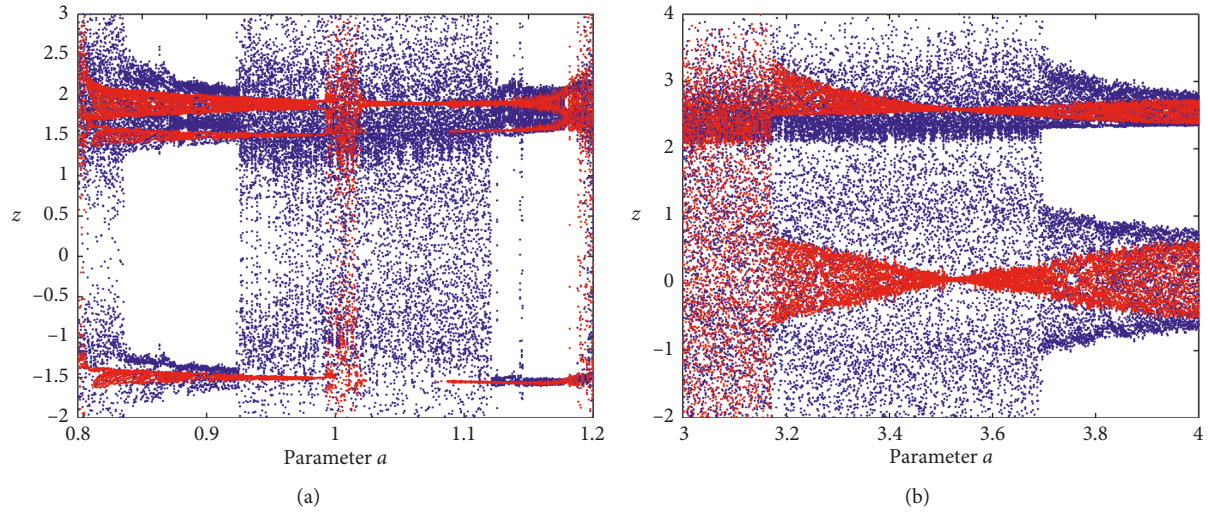


FIGURE 3: Enlargement of the bifurcation diagrams of Figure 2(a) in ranges of (a)  $[0.8, 1.2]$  and (b)  $[3, 4]$ ; the initial conditions are  $(0.1, 0, 0)$  for blue diagrams and  $(0.2, 0, 0)$  for red diagrams.

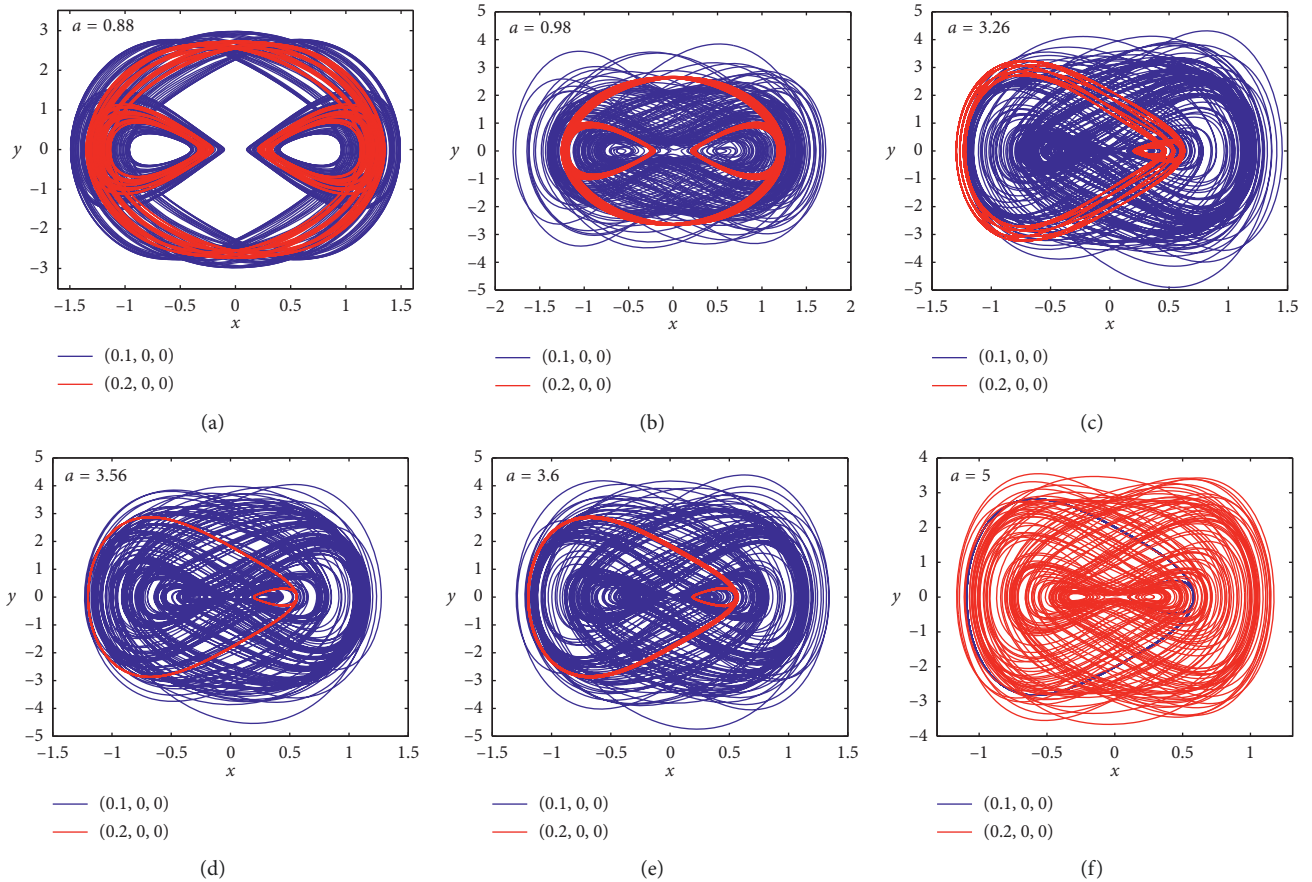


FIGURE 4: Coexistence of different attractors with different parameter  $a$ . (a) Quasiperiods with different shape; (b) chaos and quasiperiod; (c) chaos and complicated period; (d) chaos and period-1; (e) chaos and quasiperiod; (f) period and chaos, for the initial conditions  $(0.1, 0, 0)$  and  $(0.2, 0, 0)$ , respectively.

Lyapunov exponent are depicted in Figures 5(a) and 5(b), respectively. It can be found that when increasing initial value  $x(0)$  from  $-2$  to  $2$ , there emerge periodic windows embedded in the chaotic region, and the dynamics is symmetrically

distributed with respect to zero value. In fact, the dynamics is also symmetrically distributed with respect to  $y$ -axis and  $z$ -axis, as depicted by the dynamical map of  $x(0)$  versus  $y(0)$  and the dynamical map of  $y(0)$  versus  $z(0)$  in Figures 6(a)

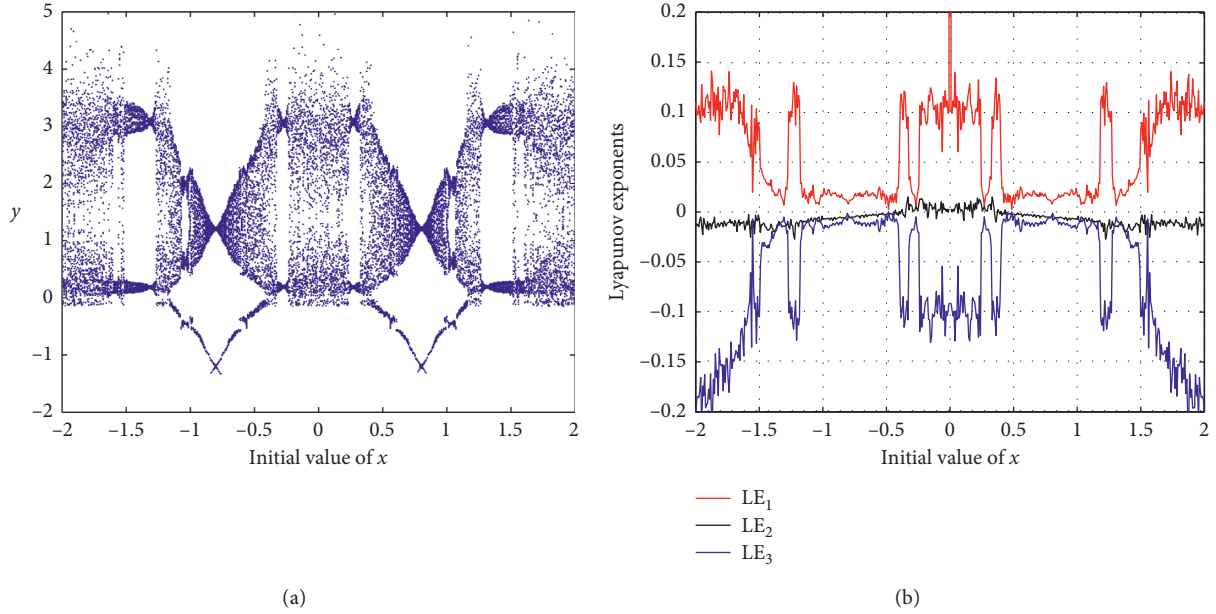


FIGURE 5: (a) Bifurcation diagram; (b) Lyapunov exponent spectrum versus  $x(0)$ .

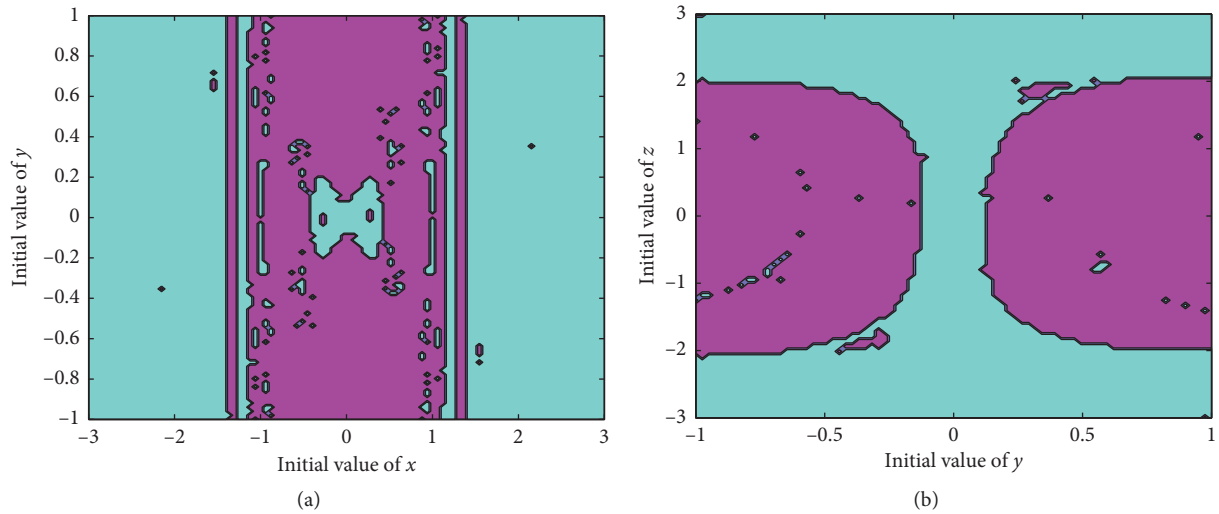


FIGURE 6: Dynamic distributions of system (1) with  $a=3$ ,  $b=-1$ ,  $c=1$ : (a)  $x(0)$  versus  $y(0)$  with  $z(0)=0$ ; (b)  $y(0)$  versus  $z(0)$  with  $x(0)=0.1$ . The chaotic regions are shown in cyan and the periodic regions are shown in pink.

and 6(b), respectively. In the dynamical map, the system is chaotic in the cyan region and periodic in the pink region. Some representative coexistence attractors of symmetric distribution with respect to  $x(0)$  are displayed in Figure 7.

**2.3. Transient Dynamics.** It is surprising to see in Figure 2(b) that a periodic window appears in the parameter region of  $2.586 \leq a \leq 2.688$ , but it does show the chaotic behavior in Figure 2(a). The emergence of different dynamical modes is due to the transition from the long term transient period to steady chaos with the time evolutions of system. The transient dynamics can be represented by chaotic orbit before entering the final nonchaotic behavior, and the inverse process is also correct.

Firstly, the case of system parameters  $a=3$ ,  $b=-1$ , and  $c=1$  and initial condition  $x(0)=0.1$ ,  $y(0)=0.15$ ,  $z(0)=0.1$  is considered. The time trajectory in the region of  $[0 \text{ s}, 800 \text{ s}]$  and the phase diagrams in two different time intervals of  $[0 \text{ s}, 400 \text{ s}]$  and  $[450 \text{ s}, 800 \text{ s}]$  are depicted in Figure 8, which illustrates the dynamics transformation from transient period to steady chaos.

Then we take the selection of system parameters  $a=3$ ,  $b=-1$ , and  $c=1$  and initial condition  $x(0)=0.3$ ,  $y(0)=0.1$ ,  $z(0)=0.6$ . The time trajectory in the region of  $[0 \text{ s}, 2000 \text{ s}]$  and the phase diagrams in two different time intervals of  $[0 \text{ s}, 900 \text{ s}]$  and  $[1100 \text{ s}, 2000 \text{ s}]$  are depicted in Figure 9. It is observed in Figure 9 that the trajectory of system (1) starts from a quasiperiodic orbit for a long time and then it transforms into a chaotic state at  $t=1050 \text{ s}$ . Similarly to transient chaos, we call this dynamic phenomenon as transient quasiperiod.

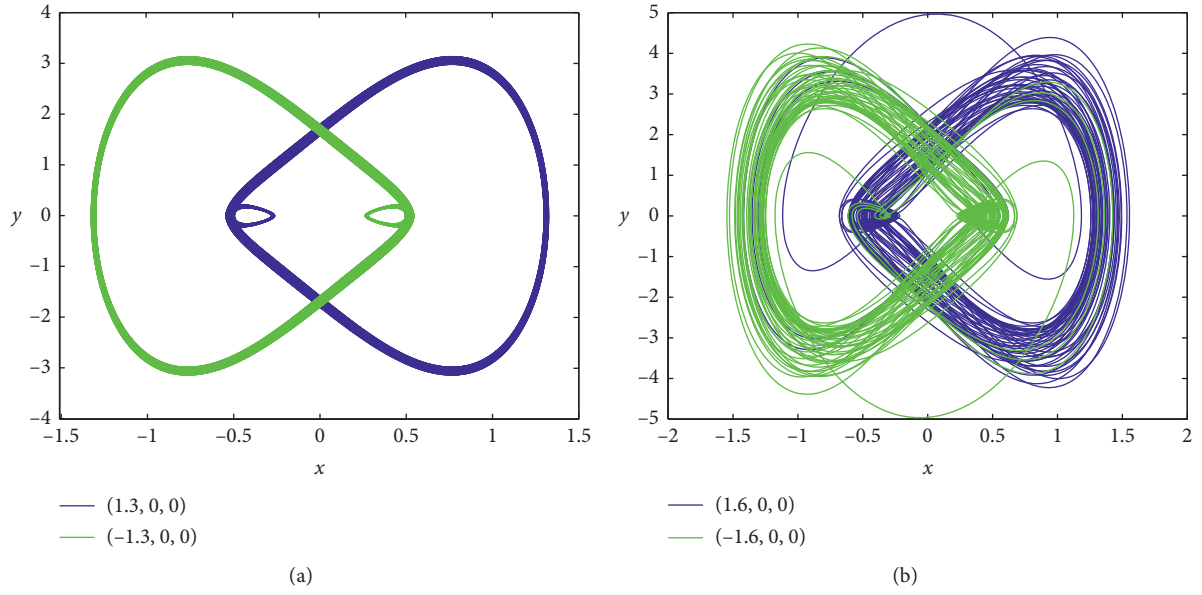


FIGURE 7: Symmetric coexisting attractors with respect to  $x(0)$ . (a) Period with  $x(0) = 1.3$  and  $-1.3$ ; (b) chaos with  $x(0) = 1.6$  and  $-1.6$ .

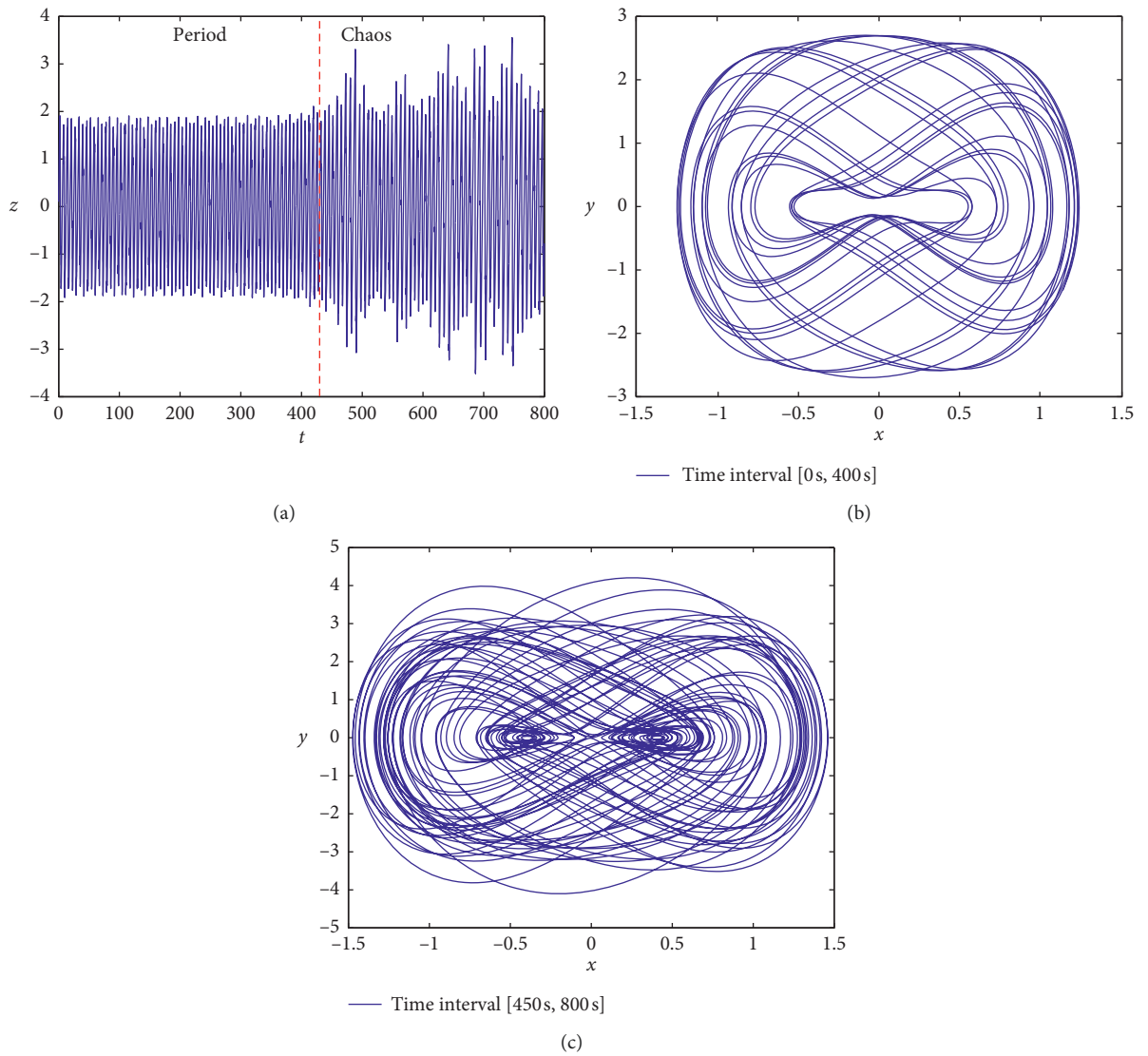


FIGURE 8: (a) Time-domain waveform of  $z$  in the region of  $[0 \text{ s}, 800 \text{ s}]$ ; (b) the phase portrait in time interval of  $[0 \text{ s}, 400 \text{ s}]$ ; (c) the phase portrait in time interval of  $[450 \text{ s}, 800 \text{ s}]$ .

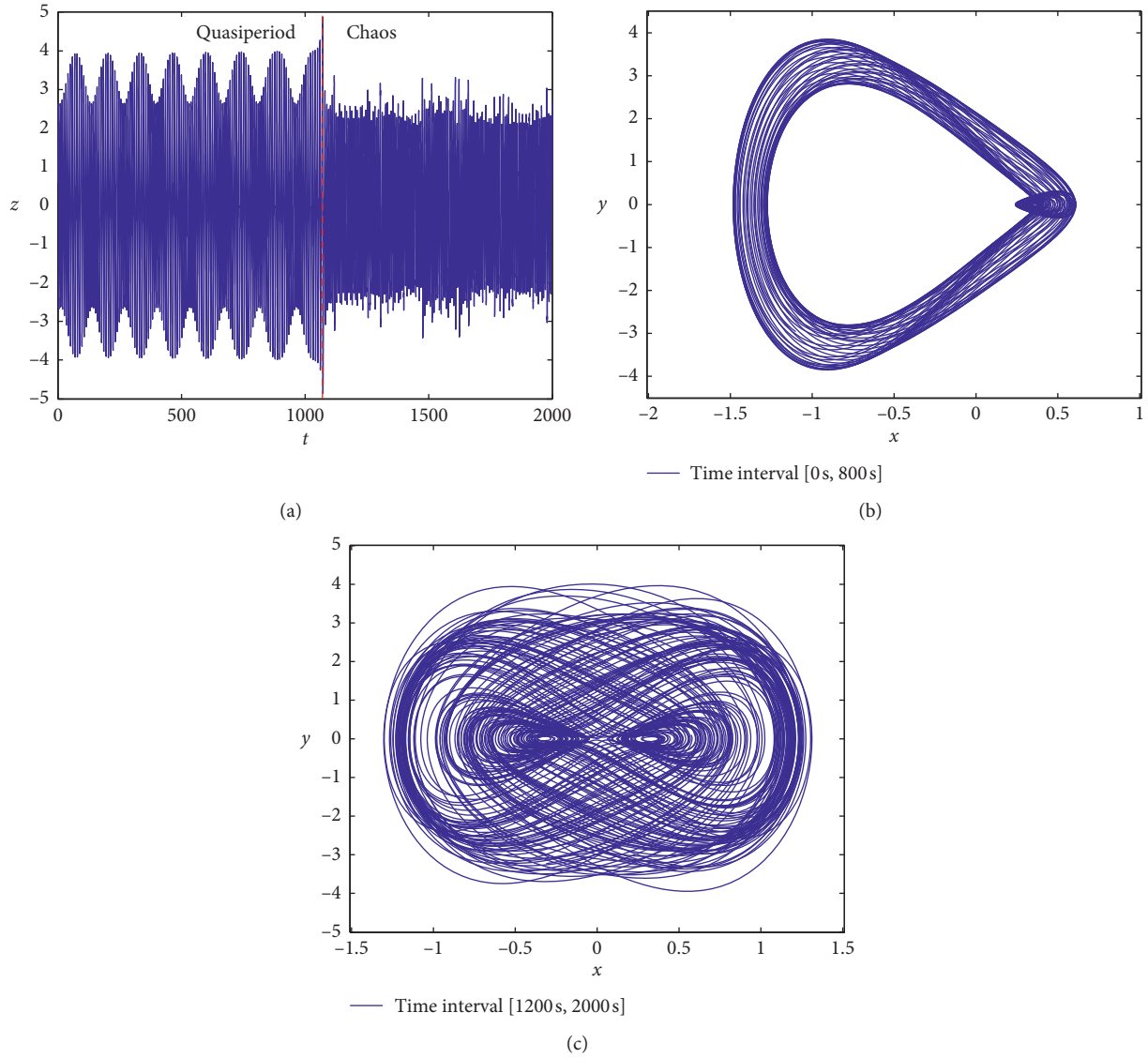


FIGURE 9: (a) Time-domain waveform of  $z$  in the region of  $[0 \text{ s}, 2000 \text{ s}]$ ; (b) the phase portrait in time interval of  $[0 \text{ s}, 900 \text{ s}]$ ; (c) the phase portrait in time interval of  $[1100 \text{ s}, 2000 \text{ s}]$ .

### 3. Synchronization Control of Memristor-Based Chaotic System

**3.1. Synchronization Scheme.** We consider the master-slave synchronization scheme for the introduced chaotic system, and the corresponding master-slave systems are described by the compact form:

$$\text{master system } \frac{dx}{dt} = f(x), \quad (2)$$

$$x = (x_1, x_2, x_3) = (x, y, z),$$

$$\text{slave system } \frac{dy}{dt} = f(y), \quad (3)$$

$$y = (y_1, y_2, y_3) = (x', y', z').$$

In which,  $f(\cdot) \in R^3$  is the smooth vector field satisfying the Lipschitz condition:

$$\begin{aligned} \|f_i(x) - f_i(y)\| &\leq k \|x_i - y_i\| \leq k \|x - y\|_\infty, \\ \|x - y\|_\infty &= \max_i \|x_i - y_i\|, \\ i &= 1, 2, 3. \end{aligned} \quad (4)$$

To realize the synchronization of systems (2) and (3), we add a single linear controller to the  $i$ -th equation of the slave system, as depicted by

$$\begin{aligned} \frac{dy}{dt} &= f(y) + u_i, \\ u_i &= \mu(x_i - y_i). \end{aligned} \quad (5)$$

The synchronization error is defined by  $e_i = x_i - y_i$ ,  $i = 1, 2, 3$ . Also, we construct the candidate Lyapunov function as  $V = (1/2) \sum_{i=1}^3 (x_i - y_i)^2$ . The time derivative of  $V$  along the synchronization error is deduced by



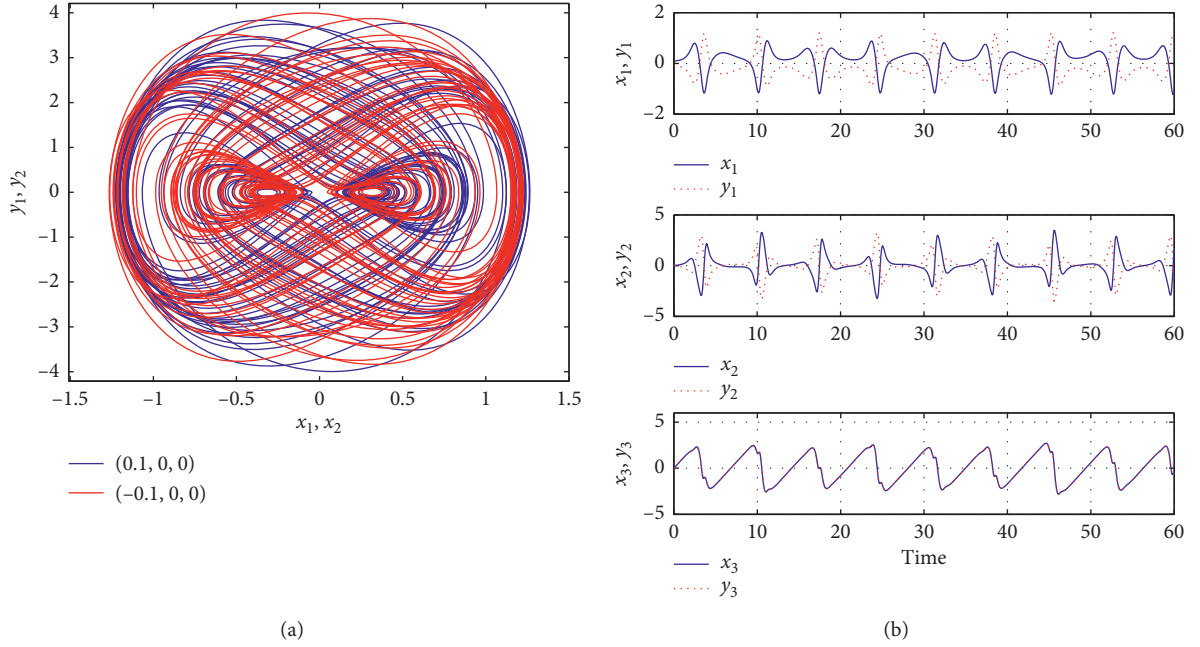


FIGURE 10: (a) Phase diagram and (b) state trajectories with  $x(0) = (0.1, 0, 0)$  and  $y(0) = (-0.1, 0, 0)$ .

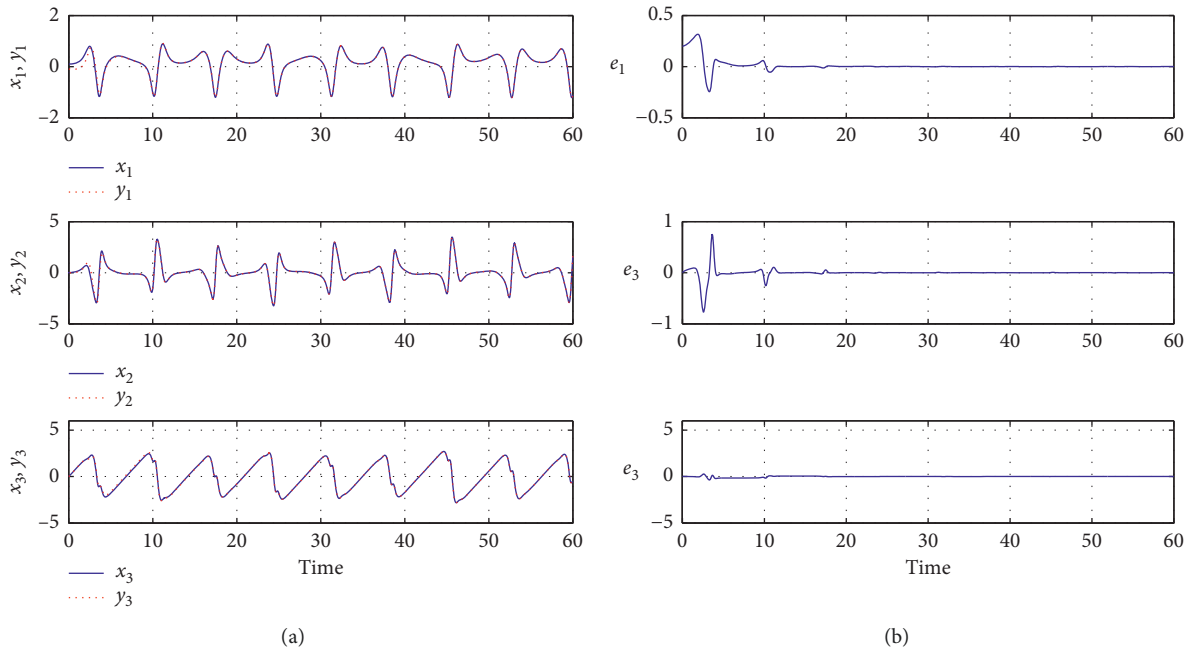


FIGURE 11: (a) Time response of the states and (b) synchronization error with  $\mu = 3$ ,  $x(0) = (0.1, 0, 0)$  and  $y(0) = (-0.1, 0, 0)$ .

$$\begin{aligned}
 \dot{V} &= \sum_{i=1}^3 (x_i - y_i)(\dot{x}_i - \dot{y}_i) \\
 &= \sum_{i=1}^3 (x_i - y_i)(f_i(x) - f_i(y) - u_i) \\
 &= \sum_{i=1}^3 (x_i - y_i)(f_i(x) - f_i(y)) - \mu \sum_{i=1}^3 (x_i - y_i)^2 \\
 &\leq (3k - \mu) \|x - y\|_{\infty}^2.
 \end{aligned} \tag{6}$$

When  $\mu \geq 3k$ , we have  $\dot{V} \leq 0$ . Thus, the controlled slave system will asymptotically synchronize with the master system with the simple controller  $u_i = \mu(x_i - y_i)$  when  $\mu \geq 3k$ .

In fact, to reduce the control consumption, we can optimize the controller as

$$u_i = \mu(x_i - y_i) \cdot H(|x_i - y_i| - \varepsilon), \tag{7}$$

where  $\varepsilon$  is a small positive constant; the function  $H(\cdot)$  is described as  $H(z) = 1$  when  $z \geq 0$  and  $H(z) = 0$  when  $z < 0$ .



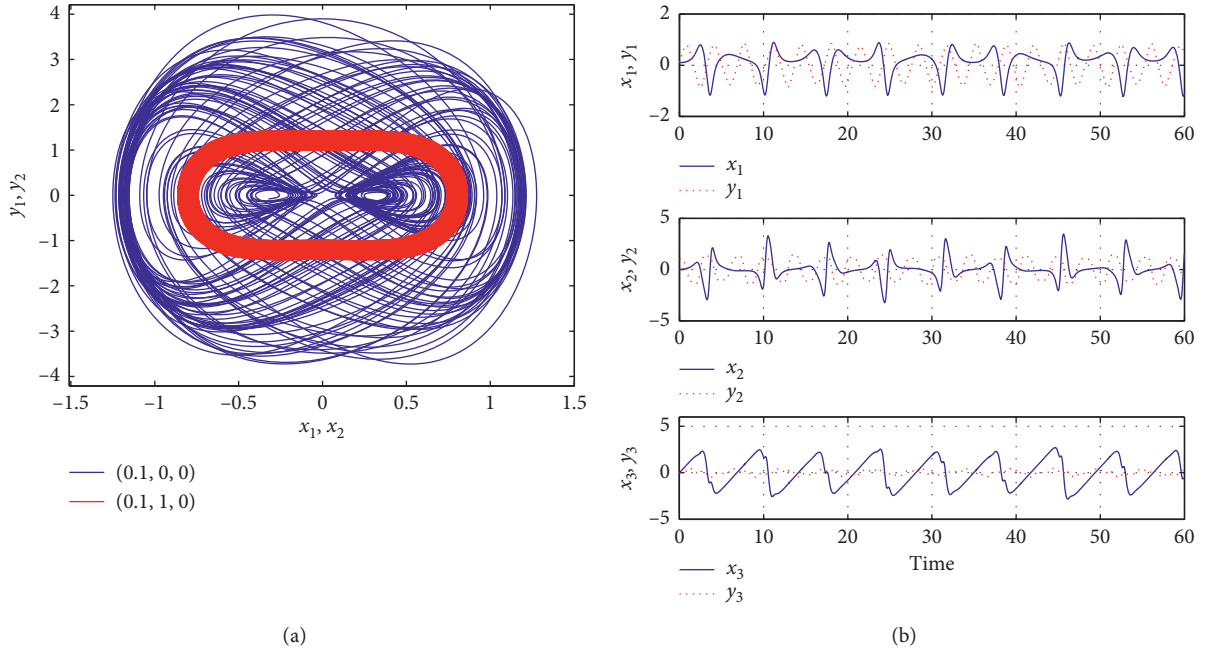


FIGURE 12: (a) Phase diagram and (b) state trajectories with  $x(0) = (0.1, 0, 0)$  and  $y(0) = (0.1, 1, 0)$ .

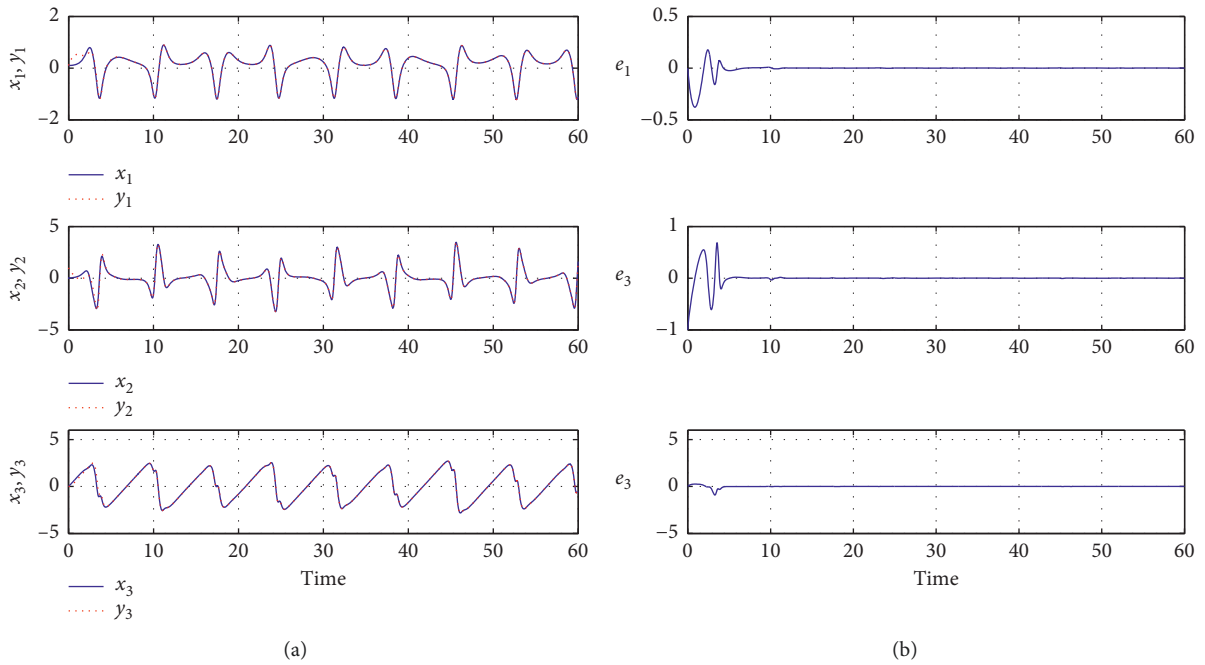


FIGURE 13: (a) Time response of the states and (b) synchronization error with  $\mu=2$ ,  $x(0) = (0.1, 0, 0)$  and  $y(0) = (0.1, 1, 0)$ .

The practical significance of the optimized control scheme is that one imposes the controller  $\mu(x_i - y_i)$  to the slave system when  $|x_i - y_i| \geq \varepsilon$ , but the controller does not work when  $|x_i - y_i| < \varepsilon$ . Thus, the controller can realize the system synchronization intermittently with the adaptive mechanism, according to the characteristics of motion trajectories. Therefore, compared with continuous synchronization schemes, intermittent synchronization will reduce the amount of conveyed information, which is of significance in the practical communication since the communication channel

capacity will be reserved for more message transmission. In addition, the security of chaotic communication system will be improved due to the reduction of redundancy of synchronization information in the channel.

**3.2. Numerical Simulation.** We impose the controller  $\mu(x_2 - y_2) \cdot H(|x_2 - y_2| - \varepsilon)$  to the second term of the slave system. The system parameters are set as  $a = 3$ ,  $b = -1$ , and  $c = 1$ .

We first choose the initial condition of system (2) as  $x(0) = (0.1, 0, 0)$  with which system (2) is chaotic, and the initial states of system (4) are taken as  $y(0) = (-0.1, 0, 0)$  for also displaying chaotic, as shown in Figure 10. The synchronization result is shown in Figure 11 when the controller gain  $\mu$  equals 3 and  $\varepsilon$  is set to be 0.02.

Then, we also set  $x(0) = (0.1, 0, 0)$  with which system (2) is chaotic, but the initial states of system (4) are taken as  $y(0) = (0.1, 1, 0)$  for displaying quasiperiodic, as shown in Figure 12. The synchronization result is shown in Figure 13 when controller parameters  $\mu = 2$  and  $\varepsilon = 0.02$ .

We know that no matter what the dynamic state of the memristive system is, the synchronization control of the memory system can be easily realized by adopting the designed method.

#### 4. Conclusions

In this paper, we introduce a memristor-based chaotic system with no equilibrium. Various tools including phase diagram, time-domain trajectory, bifurcation diagram, and Lyapunov exponent are exploited to establish the connection between the system parameters and dynamical behaviors. It is found that the reported system exhibits complex dynamics such as coexisting bifurcation, multistability, symmetric coexisting attractors, and transient dynamics, which is helpful for the security improvement of encryption and communication due to the difficulty of reproducing the accurate dynamics. Then, a simple control scheme with single linear couple is developed to achieve complete synchronization for the memristive system. Since the output signal is transmitted intermittently to the receiver system with the adaptive mechanism, the communication channel capacity will be reserved for more message transmission. Also, the security of chaotic communication system will be improved for the reduction of redundancy of synchronization information in the channel.

#### Data Availability

The data used to support the findings of this study are included within the article.

#### Conflicts of Interest

The authors declare that there are no conflicts of interest regarding the publication of this paper.

#### Acknowledgments

This work was supported by the Hunan Provincial Natural Science Foundation of China (no. 2019JJ40109); Research Foundation of Education Bureau of Hunan Province of China (no. 18A314); and Science and Technology Program of Hunan Province (no. 2016TP1021).

#### References

- [1] L. Chua, "Memristor-the missing circuit element," *IEEE Transactions on Circuit Theory*, vol. 18, no. 5, pp. 507–519, 1971.

- [2] D. B. Strukov, G. S. Snider, D. R. Stewart, and R. S. Williams, "The missing memristor found," *Nature*, vol. 453, no. 7191, pp. 80–83, 2008.
- [3] Q. Zhao, C. Wang, and X. Zhang, "A universal emulator for memristor, memcapacitor, and meminductor and its chaotic circuit," *Chaos: An Interdisciplinary Journal of Nonlinear Science*, vol. 29, no. 1, Article ID 013141, 2019.
- [4] V.-T. Pham, S. Vaidyanathan, C. K. Volos, S. Jafari, N. V. Kuznetsov, and T. M. Hoang, "A novel memristive time-delay chaotic system without equilibrium points," *The European Physical Journal Special Topics*, vol. 225, no. 1, pp. 127–136, 2016.
- [5] D. Ma, G. Wang, C. Han, Y. Shen, and Y. Liang, "A memristive neural network model with associative memory for modeling affections," *IEEE Access*, vol. 6, pp. 61614–61622, 2018.
- [6] H. Bao, N. Wang, H. Wu, Z. Song, and B. Bao, "Bi-stability in an improved memristor-based third-order Wien-bridge oscillator," *IETE Technical Review*, vol. 36, no. 2, pp. 109–116, 2019.
- [7] F. Corinto and M. Forti, "Memristor circuits: bifurcations without parameters," *IEEE Transactions on Circuits and Systems I: Regular Papers*, vol. 64, no. 6, pp. 1540–1551, 2017.
- [8] M. Itoh and L. O. Chua, "Memristor oscillators," *International Journal of Bifurcation and Chaos*, vol. 18, no. 11, pp. 3183–3206, 2008.
- [9] T. F. Fonzin, K. Srinivasan, J. Kengne, and F. B. Pelap, "Coexisting bifurcations in a memristive hyperchaotic oscillator," *AEU-international Journal of Electronics and Communications*, vol. 90, pp. 110–122, 2018.
- [10] X. Bi-Rong, "A simplest parallel chaotic system of memristor," *Acta Physica Sinica*, vol. 62, no. 19, pp. 99–106, 2013.
- [11] Y. Zhao, Y. Jiang, J. Feng, and L. Wu, "Modeling of memristor-based chaotic systems using nonlinear Wiener adaptive filters based on backlash operator," *Chaos, Solitons & Fractals*, vol. 87, pp. 12–16, 2016.
- [12] L. Teng, H. H. C. Iu, X. Wang, and X. Wang, "Chaotic behavior in fractional-order memristor-based simplest chaotic circuit using fourth degree polynomial," *Nonlinear Dynamics*, vol. 77, no. 1-2, pp. 231–241, 2014.
- [13] M. Guo, W. Yang, Y. Xue et al., "Multistability in a physical memristor-based modified Chua's circuit," *Chaos: An Interdisciplinary Journal of Nonlinear Science*, vol. 29, no. 4, Article ID 043114, 2019.
- [14] Y.-B. Zhao, C.-K. Tse, J.-C. Feng, and Y.-C. Guo, "Application of memristor-based controller for loop filter design in charge-pump phase-locked loops," *Circuits, Systems, and Signal Processing*, vol. 32, no. 3, pp. 1013–1023, 2013.
- [15] G. Peng and F. Min, "Multistability analysis, circuit implementations and application in image encryption of a novel memristive chaotic circuit," *Nonlinear Dynamics*, vol. 90, no. 3, pp. 1607–1625, 2017.
- [16] X. Hu, S. Duan, L. Wang, and X. Liao, "Memristive crossbar array with applications in image processing," *Science China Information Sciences*, vol. 55, no. 2, pp. 461–472, 2012.
- [17] W. Wang, X. Yu, X. Luo, and J. Kurths, "Synchronization control of memristive multidirectional associative memory neural networks and applications in network security communication," *IEEE Access*, vol. 6, pp. 36002–36018, 2018.
- [18] V.-T. Pham, A. Akgul, C. Volos, S. Jafari, and T. Kapitaniak, "Dynamics and circuit realization of a no-equilibrium chaotic system with a boostable variable," *AEU—International Journal of Electronics and Communications*, vol. 78, pp. 134–140, 2017.

- [19] S. Jafari, A. Ahmadi, A. J. M. Khalaf, H. R. Abdolmohammadi, V.-T. Pham, and F. E. Alsaadi, "A new hidden chaotic attractor with extreme multi-stability," *AEU—International Journal of Electronics and Communications*, vol. 89, pp. 131–135, 2018.
- [20] D. Cafagna and G. Grassi, "Chaos in a new fractional-order system without equilibrium points," *Communications in Nonlinear Science and Numerical Simulation*, vol. 19, no. 9, pp. 2919–2927, 2014.
- [21] G. A. Leonov, N. V. Kuznetsov, and V. I. Vagitsev, "Hidden attractor in smooth Chua systems," *Physica D: Nonlinear Phenomena*, vol. 241, no. 18, pp. 1482–1486, 2012.
- [22] S. Jafari and J. C. Sprott, "Simple chaotic flows with a line equilibrium," *Chaos, Solitons & Fractals*, vol. 57, pp. 79–84, 2013.
- [23] Z. Wei and Q. Yang, "Dynamical analysis of the generalized Sprott C system with only two stable equilibria," *Nonlinear Dynamics*, vol. 68, no. 4, pp. 543–554, 2012.
- [24] X. Wang and G. Chen, "A chaotic system with only one stable equilibrium," *Communications in Nonlinear Science and Numerical Simulation*, vol. 17, no. 3, pp. 1264–1272, 2012.
- [25] V.-T. Pham, S. Jafari, C. Volos, A. Giakoumis, S. Vaidyanathan, and T. Kapitaniak, "A chaotic system with equilibria located on the rounded square loop and its circuit implementation," *IEEE Transactions on Circuits and Systems II: Express Briefs*, vol. 63, no. 9, pp. 878–882, 2016.
- [26] V.-T. Pham, C. Volos, S. Jafari, S. Vaidyanathan, T. Kapitaniak, and X. Wang, "A chaotic system with different families of hidden attractors," *International Journal of Bifurcation and Chaos*, vol. 26, no. 8, Article ID 1650139, 2016.
- [27] L. M. Pecora and T. L. Carroll, "Synchronization in chaotic systems," *Physical Review Letters*, vol. 64, no. 8, pp. 821–824, 1990.
- [28] C. Li, "Tracking control and generalized projective synchronization of a class of hyperchaotic system with unknown parameter and disturbance," *Communications in Nonlinear Science and Numerical Simulation*, vol. 17, no. 1, pp. 405–413, 2012.
- [29] H. Sang and J. Zhao, "Exponential synchronization and  $L_2$ -gain analysis of delayed chaotic neural networks via intermittent control with actuator saturation," *IEEE Transactions on Neural Networks and Learning Systems*, pp. 1–13, 2019.
- [30] C. Yang, L. Huang, and Z. Cai, "Fixed-time synchronization of coupled memristor-based neural networks with time-varying delays," *Neural Networks*, vol. 116, pp. 101–109, 2019.
- [31] C. Li, Y. Tong, H. Li, and K. Su, "Adaptive impulsive synchronization of a class of chaotic and hyperchaotic systems," *Physica Scripta*, vol. 86, no. 5, Article ID 055003, 2012.
- [32] R. G. Li and H. N. Wu, "Adaptive synchronization control with optimization policy for fractional-order chaotic systems between 0 and 1 and its application in secret communication," *ISA transactions*, vol. 92, pp. 35–48, 2019.
- [33] W. G. Hoover, "Remark on 'Some simple chaotic flows'," *Physical Review E*, vol. 51, no. 1, pp. 759–760, 1995.

